BJES Basrah Journal for Engineering Sciences

Basrah Journal for Engineering Sciences, Vol. 22, No. 1, (2022), 20-28

Original Article

Journal homepage: www.bjes.edu.iq
ISSN (Online): 23118385, ISSN (Print): 18146120

OPEN ACCESS

Numerical Study Mixed Convection in a Channel with an Open Cavity Involving Rotary Cylinder

Eman G. Mohammed [1,*], Falah A. Abood [2]

[1,2] *Department of Mechanical Engineering, College Engineering, University of Basrah, Basrah, Iraq*
E-mail addresses: eman.ghazi1995@gmail.com , falahass123@gmail.com
Received: 28 October 2021; Accepted: 16 November 2021; Published: 24 April 2022

Abstract

A numerical study of mixed convection inside a horizontal channel with an open square cavity that includes an adiabatic rotating cylinder. The bottom wall of the cavity is heated at a constant temperature, and the remaining walls are adiabatic. The flow is incompressible, laminar and steady state. The equations of continuity, momentum and energy are solved numerically using computational fluid dynamics (CFD) with the commercial software package FLUENT 2019 R1. Reynolds number values of 50, 100 and 150, the Richardson number ($0.1 \leq Ri \leq 10$) and the angular velocity (ω) of cylinder is ($0.5 \leq \omega \leq 4$) rad/sec with direction counter clockwise. Prandtl number for air flow is ($Pr = 0.7$). The results are presented in terms of streamlines, isotherms, and the average Nusselt value is given over the heated bottom cavity. The combined effects of natural and forced convection in and out of the cavity were obtained. The results showed that at low Richardson values, $Ri = 0.1$ the effect of buoyancy force is neglected. The effect of increasing the cylinder speed is clearly noticeable at low Reynolds values, $Re = 50$. Average Nusselt values increase with increasing rotational speed of the cylinder for all Richardson values.

Keywords: Mixed convection, Laminar flow, Channel, Square cavity, Rotating cylinder.

http://dx.doi.org/10.33971/bjes.22.1.3

1. Introduction

The flow structure over an open cavity has been a commonly studied topic in recent decades, due to its importance in a variety of engineering applications and practical devices [1], [2], also including fuselages, harbor entrances, bomb bays, solar collectors, nuclear reactor and electronic part cooling. Many studies have looked at heat transfer with mixed convection in cavities of various forms that contain a heat conducting object, an adiabatic item that is either fixed or moving, and cavities that contain nothing.

Manca et al. (2003) [3] investigated the effect of heat wall location on mixed convection in a channel with an open cavity and discovered that when the Reynolds number and Richardson number increase, the maximum temperature values decrease for all of the configurations evaluated.

Stiriba et al. (2010) [4] examined numerically the flow and heat transfer characteristics of incompressible laminar flow past an open cavity. For $Re = 100$ with Ri ranging from 0.01 to 10 and $Re = 1000$ with Ri ranging from 0.001 to 1, the results show that the flow has a three-dimensional structure and is steady. The forced flow dominates the flow transport mechanism, and there is a large recirculating zone inside the enclosure, resulting in heat transfer by conduction.

Abdelmassih et al. (2012) [5] and experimental (2013) [6] used a finite volume flow solver to present a three-dimensional numerical simulation study for both laminar steady and unsteady flow to interpret the mixed convective over a three-dimensional cubical open cavity. The bottom of the cavity was heated at constant temperature while the other walls are adiabatic. The range of Reynolds numbers is $100 \leq Re \leq 1500$, Prandtl number (Pr) for air flow is set equal to 0.7 and Richardson number range is $0.001 \leq Ri \leq 10$. The results show that, for both high Re and Ri the flow becomes unsteady. The mixed convection effects dominate the flow transport mechanism and push the recirculation zone and the flow further upstream. Rahman et al. (2008) [7] used finite element method to present numerical simulation for steady laminar mixed convection flow within a vented square cavity with a heat conducting horizontal solid circular cylinder mounted at the center of the cavity. The Richardson number is varied from 0.0 to 5.0, and the cylinder diameter is varied from 0.0 to 0.6. The results revealed that the Richardson number and cylinder diameter have a significant influence on streamlines, isotherms, average Nusselt number at the heated surface, average temperature of the fluid in the cavity, and dimensionless temperature at the cylinder core.

Khanafer et al. (2013) [8] studied a moving wall cavity with a central cylinder for laminar combined convection heat transfer and flow patterns. The cylinder body within the cavity was found to be able to control the heat transfer fields. The heat transmission and flow properties might be affected by the size and placement of the obstruction.

Costa et al. (2010) [9] studied combined convection of heat transfer and fluid structure of a 2D differentially heated square cavity containing a central rotating cylinder which has been simulated numerically. Investigated the effects of the rotating cylinder size and rotational speed. It was demonstrated that discernible influences on the heat transfer and fluid characteristics have been noticed by changing either the cylinder size or its rotation speed.

Sachin et al. (2009) [10] Numerical studied for Reynolds numbers of 20-160 and a Prandtl number of 0.7, forced convection heat transfer across a circular cylinder rotating with a constant non-dimensional rotation rate a varied from 0 to 6 is examined. Flow transitions over a larger range of Reynolds numbers and rotation rates are reported here. The average Nusselt number is observed to drop with rising rotation rate and increase with rising *Re*, achieving a near-constant value for all *Re* at the maximum rotation rate. with increasing *Re* and increasing rotation rate, heat transfer suppression due to rotation increases.

Salam et al. (2011) [11] in this study, a numerical simulation of a laminar stable mixed convection issue in a two-dimensional square enclosure of width and height (L) with a revolving circular cylinder of radius (R = 0.2 L) enclosed inside it is carried out using a finite volume technique. For Richardson numbers of 0, 1, 5, and 10, as well as Reynolds numbers of 50, 100, 200, and 300. Increases in the Richardson and Reynolds numbers have a substantial impact on the flow and temperature fields, and rotating cylinder placements have a substantial impact on increasing convection heat transfer in the square enclosure, according to the findings of this study.

Selimefendigil et al. (2014) [12] investigated numerically the heat transfer enhancement and fluid flow properties of a rotating cylinder in the backward facing step geometry under the effect of magnetic dipole. The effects of Reynolds number ($10 \le Re \le 200$) and cylinder rotation angle ($-75 \le \Omega \le 75$) and the effect of the magnetic dipole strength ($0 \le \gamma \le 16$). A commercial solver based on finite elements is used to solve the governing equations. The local Nusselt number rises as the Reynolds number rises, and the number of peaks in the presence of the magnetic field decreases. At low Reynolds numbers, the effect of cylinder rotation on the local Nusselt number distribution is more pronounced.

Chatterjee et al. (2014) [13] investigated numerically a 2D mixed convective transport in a moving top wall cavity that includes a thermal adiabatic central rotating circular cylinder and this enclosure was filled by Cu-water Nano fluid. It was observed that the forced convection was dominated on the fluid flow and the heat transfer at the low value of the *Ri* number. By contrast, the natural convection has the main effect on the heat transfer and fluid at a high *Ri* number. The drag coefficient of the moving lid-driven wall incremented by increasing the speed of the rotating cylinder and by increasing the *Ri* number. Thus, increasing *Ri* enhances the Nusselt number on the heated wall. The previous research included studying the process of heat transfer by mixed convection within horizontal channels that include open cavities in addition to a lid driven cavity that may contain a fixed or rotation cylinder are numerically studied. In this study, the effects of rotation under mixed convection inside a horizontal channel with an open square cavity including a rotating cylinder on heat transfer enhancement and fluid flow characteristics are investigated numerically. For convective heat transfer enhancement over a square open cavity flow, the effects of various parameters such as Reynolds number, Richardson number, and cylinder rotation speed are examined.

2. Theoretical Analysis

2.1. Geometry Description

The geometry of the channel including the square open cavity contains a rotating cylinder at its center and the computational domain used in this study are shown in Fig. 1.

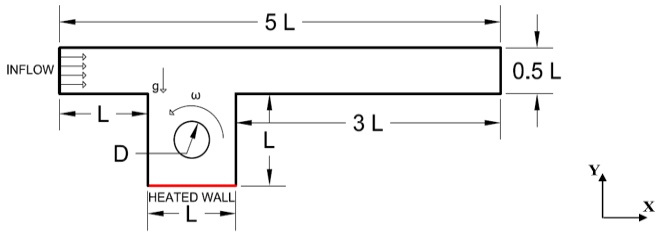

Fig.1 Sketch of the geometry.

Where L is the length (L = 0.1 m). The length of the channel from the inlet opening to the cavity leading edge is L, while 3L is the length of the channel behind the cavity trailing edge in the streamwise direction, the height of the channel is 0.5 L, and D is a diameter of cylinder. The inflow direction is from left to right with a uniform velocity U_0 and a constant temperature T_∞ at x = 0. Outflow boundary condition is assumed, located at x = 5 L and the non-slip boundary condition is applied for the rest of the boundaries. The cavity is heated from below at a constant temperature, and the remaining walls of the cavity, cylinder and the channel are adiabatic. Prandtl number for air flow (Pr = 0.7). The Reynolds number range is set ($50 \le Re \le 150$), while the Richardson number range is ($0.1 \le Ri \le 10$). The thermo-physical properties of air flow are assumed to be constant, except for the change in fluid density with temperature according to the Boussinesq approximation.

2.2. Mathematical Modeling

The Navier-Stokes equations for mass, momentum, and energy conservations based on the preceding assumptions in the Cartesian coordinates are the following:

Continuity equation:

$$\frac{\partial u}{\partial x} + \frac{\partial v}{\partial y} = 0 \tag{1}$$

Momentum equations can be written as:

X-momentum equation:

$$u\frac{\partial u}{\partial x} + v\frac{\partial u}{\partial y} = -\frac{1}{\rho}\frac{\partial p}{\partial x} + \frac{\mu}{\rho}\left(\frac{\partial^2 u}{\partial x^2} + \frac{\partial^2 u}{\partial y^2}\right) \tag{2}$$

Y-momentum equation:

$$u\frac{\partial v}{\partial x} + v\frac{\partial v}{\partial y} = -\frac{1}{\rho}\frac{\partial p}{\partial y} + \frac{\mu}{\rho}\left(\frac{\partial^2 v}{\partial x^2} + \frac{\partial^2 v}{\partial y^2}\right) + \rho\,\beta\,(T - T_{in}) \tag{3}$$

Energy equation for fluid:

$$u\frac{\partial T}{\partial x} + v\frac{\partial T}{\partial y} = \frac{k}{\rho\, C_p}\left(\frac{\partial^2 T}{\partial x^2} + \frac{\partial^2 T}{\partial y^2}\right) \tag{4}$$

Boundary Conditions:

1. At the inlet:

u refers to the inflow velocity components, $u = ui$, $\upsilon = 0$, $T = Ti$

2. At the exit:

$$\frac{\partial u}{\partial x} = 0, P = 0$$

3. Wall thermal condition:

The cavity is heated from below at a constant temperature T_h, T_h = constant

4. Adiabatic rotating cylinder

The angular velocity (ω) is (0.5, 2, 4) rad/s with direction counter clockwise (negative), Heat flux = 0

5. The other walls:

The remaining walls of the cavity and channel are adiabatic $u = 0$, $\upsilon = 0$, Heat flux = 0

Dimensionless Parameters:

1. Reynolds Number

$$Re = \frac{\rho\, u\, D_h}{\mu}$$

2. Grashof Number

$$Gr = \frac{g\,\beta\,(T_h - T_\infty)\,L^3}{\upsilon^2}$$

3. Richardson Number

$$Ri = \frac{Gr}{Re^2}$$

4. Prandtl Number

$$Pr = \frac{\upsilon}{\alpha}$$

Thermal parameters:

The computation of the local Nusselt number is based on the cavity height L:

$$Nu_L = -\frac{L}{\Delta T}\frac{\partial T}{\partial y}\Big|_{wall} \quad (5)$$

Where, $\Delta T = T_{hot} - T_{bulk}$

The average Nusselt number at the bottom wall is:

$$\overline{Nu} = \frac{1}{L}\int_0^L Nu_L\, dx \quad (6)$$

3. Numerical method and validation of the present calculation

The results obtained using ANSYS-FLUENT, an independent approach (2019 R1). Grid refinement tests for 2D situations show that a grid size of about 54048 triangular elements is suitable for accuracy and resolution. To ensure mass conservation and avoid pressure-velocity decoupling, the Simple Method for Pressure-Linked Equations (SIMPLE) was used. To reach the aim of convergence acceleration, all residuals were subjected to a convergence criterion of 10^{-6}. A computational model is validated by comparing the present result of *Nu* with the results presented by Burgos et al. [14].

Table 1. Comparison of the average Nusselt number (along the square) body with the results presented by Burgos et al.

Parameter, Ri	Present study, Nu	Burgos et al., Nu	Error (%)
0.01	1.283	1.347	4.75
0.1	1.514	1.507	0.46
1	2.559	2.586	1.04
10	4.034	4.202	3.99

4. Results and discussions

For various values of the dimensionless parameter *Ri*, *Re*, and dimensional angular velocity, the findings, which are displayed as streamlines and isotherms contours together with the Nusselt number, are presented and analyzed in this section. The mixed convection phenomenon in a channel cavity assembly is caused by the combined effect of forced convection, or shear force, caused by air flow inside the channel and rotating cylinder inside cavity, and natural convection, or buoyancy force, caused by the temperature gradient between the cold air flow and the local heat source embedded at the bottom wall of the cavity.

4.1. Flow field and isotherms

4.1.1. Effect of Richardson number

Figure 2 presents the streamline distribution for a channel with a square cavity containing a circular cylinder when *Re* = 50 and ω = 0.5 rad/sec. This figure shows that for *Ri* = 0.1, streamlines converged at the cylinder wall and vortex developed in the left upper part of the cavity. This suggests a high force convection effect and a low natural convection effect (negligible effect). For *Ri* = 1, the buoyant force begins with a little effect on the movement of the streamlines (effective on mixed convection). When *Ri* is increased to 10 (i.e. *Ri* = 10), the streamlines are distributed almost uniformly throughout the cavity, and their intensity increases near the cylinder wall, natural convection has more effective on mixed convection. Figure 3 presents the distribution of the isotherms contour. For *Ri* = 0.1 and 1 the isotherm lines curve towards the right part of the cavity, when the Richardson number is low, the forced convection situation is present, because the buoyancy force effect is minor, the natural convection contribution is small in this case. As the Richardson number (*Ri*) rises as *Ri* = 10, the isotherms from the heated wall become increasingly decreased, indicating diffusion heat transfer in the cavity with effect of rotating cylinder. The temperature distribution exceeds the top of the cavity and reaches the outflow region. By increasing the rotational speed of the cylinder to 4 rad/sec Fig. 4, 5. Noticed the disappearance

of the vortices for all Richardson values, and forced convection dominated the heat transfer process at low Richardson number. In addition to the improvement of the temperature contour Fig. 5 compared to the rotational speed of the previous case when ω = 0.5 rad/sec.

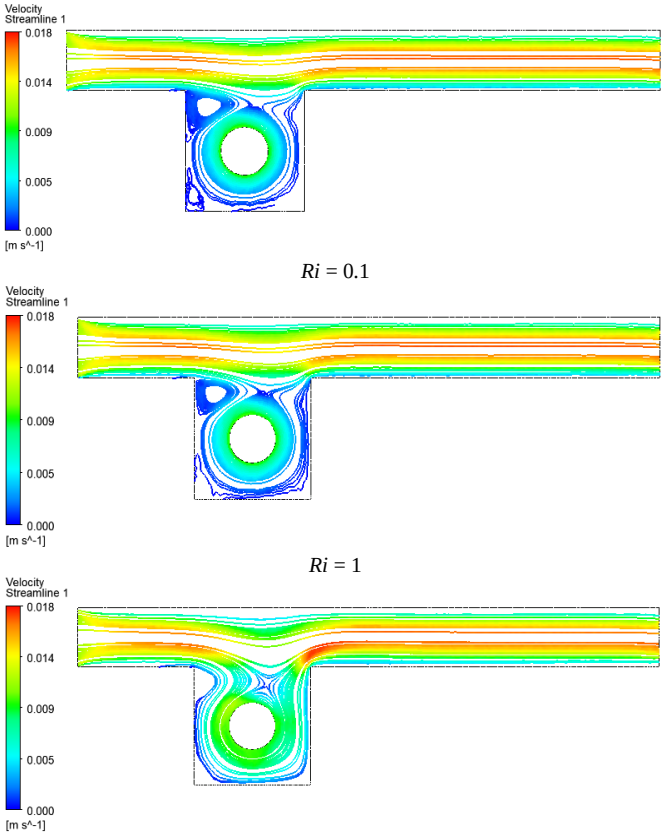

Ri = 0.1

Ri = 1

Ri = 10

Fig. 2 Streamlines contours at *Re* = 50, ω = 0.5 rad/sec.

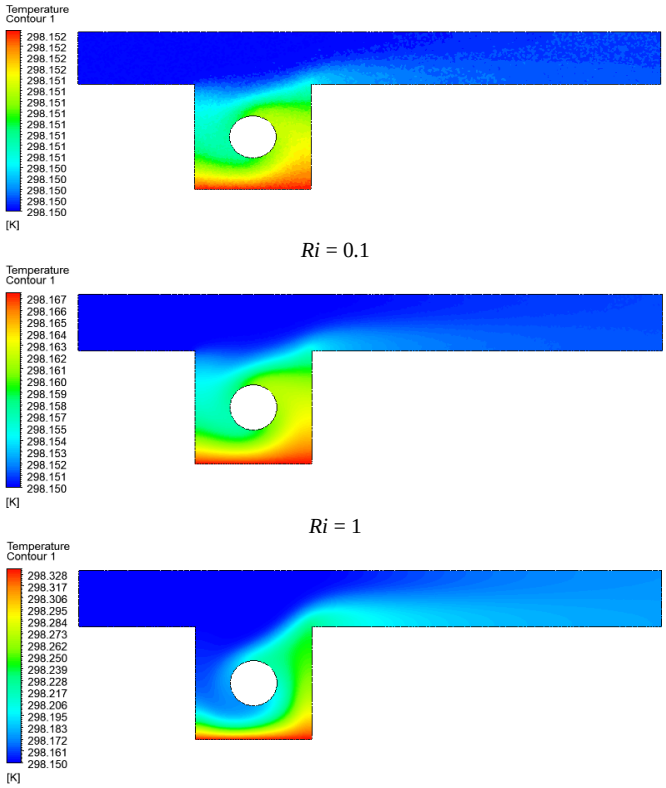

Ri = 0.1

Ri = 1

Ri = 10

Fig. 3 Isothermal contours at *Re* = 50, ω = 0.5 rad/sec.

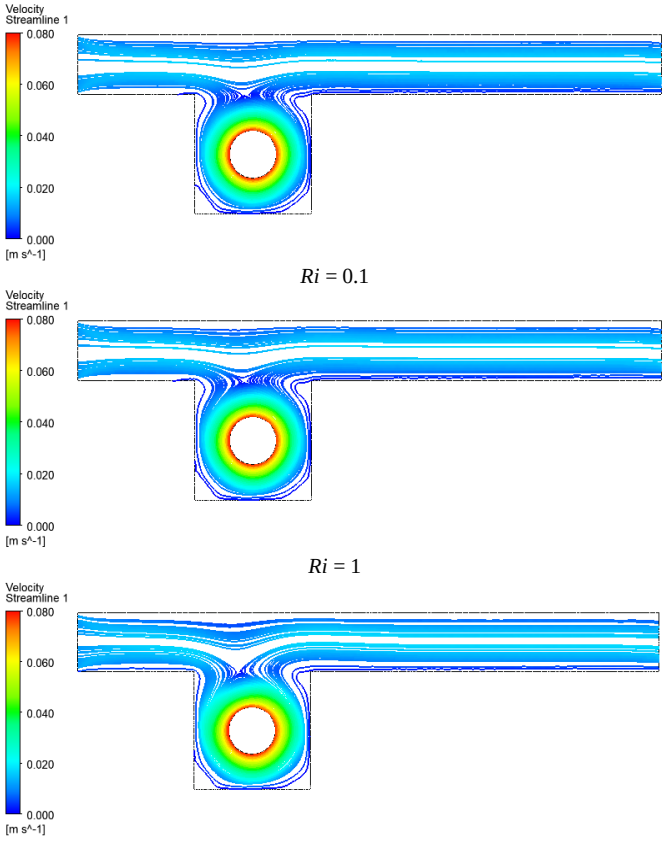

Ri = 0.1

Ri = 1

Ri = 10

Fig. 4 Streamlines contours at *Re* = 50, ω = 4 rad/sec.

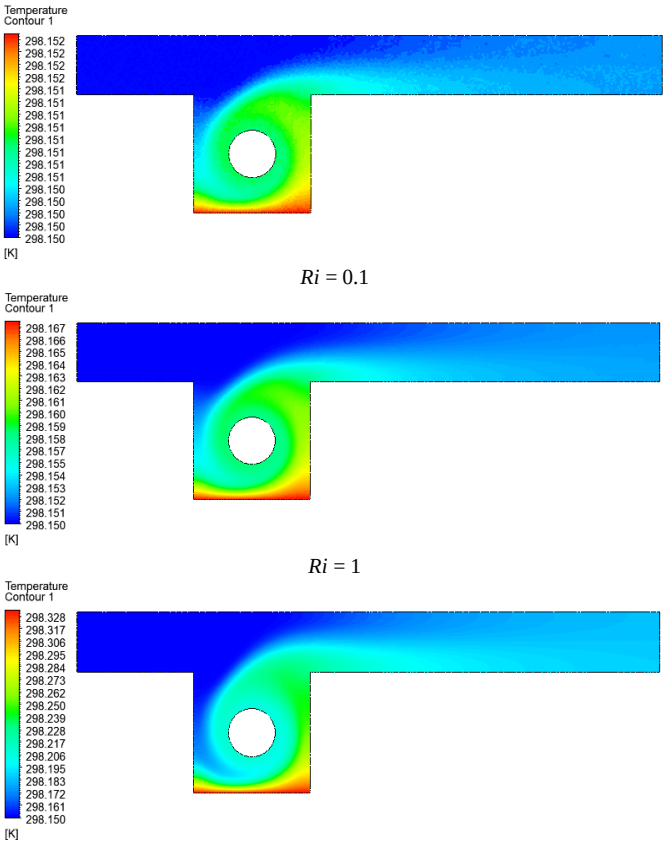

Ri = 0.1

Ri = 1

Ri = 10

Fig. 4 Isothermal contours at *Re* = 50, ω = 4 rad/sec.

4.1.2. Effect of Reynolds number

Figure 6 presents the streamline distribution for a channel with a square cavity containing a circular cylinder when *Re* = 0.1, for (*Re* = 50, 100, 150 and ω = 0.5 rad/sec). For *Re* = 50, streamlines are increasing around the cylinder wall with a vortex appearance at the top of the left of the cavity as a result of overlapping streamlines resulting from the inflow and the cylinder movement, and beginning a small vortex at the bottom of the cavity. For *Re* = 100, The vortex was observed at the top of the cavity and on its right side a small vortex was appeared, due to the effect of forced convection. With increase *Re* to 150 streamlines are centered around the cylinder wall, the interaction of streamlines is limited in the top half of the cavity. Also force convection dominated because effect of buoyant force neglected. For isotherm profile Fig. 7, noted only distribution the temperature within the cavity only, depends on the motion of the cylinder without observing the effect of increase Reynolds values. By increasing the angular velocity of the cylinder ω = 4 rad/sec, Figs. 8 and 9. Fig. 8 streamlines when (*Ri* = 0.1, ω = 4 rad/s), force convection dominated. For *Re* = 50, the flow lines are distributed approximately equal density within the cavity, and their intensity increases as they approach the cylinder wall. For *Re* = 100, the intensity of the flow lines increases towards the cylinder wall, in addition to the formation of a small vortex on the left-bottom corner of the cavity. With increase Reynolds to 150, density of the streamlines around the wall of the cylinder with the formation of vortices, one in the upper left and the other lower left corner of the cavity. The mechanism of distributing streamlines inside a cavity is regulated as a result of the increase in the forced convection (rotation of cylinder), we notice an improvement in the heat transfer process. Through the contour of the temperature Fig. 9, we notice an improvement in the heat transfer process when the Reynolds value is increased from 50 to 100, and the heat transfer efficiency decreases from 100 to 150. In comparison with the first and second rotational speeds, we notice an improvement in the heat transfer process by increasing the rotational speed of the cylinder with the change in Reynolds values.

4.1.3. Effect of rotation cylinder

Figures 10 and 11 show the effect of changing cylinder rotation on streamlines and isotherms for fixed values of *Re* = 50 and *Ri* = 1. The situation represented in Fig 10. Vortex appear behind the step for ω = 0.5 rad/sec, the density of the streamlines is centered around the cylinder wall. By increasing the rotational speed of the cylinder to (ω = 2, 4 rad/sec). Noticed the disappearance of eddies and the increase in the intensity of the streamlines in most parts of the cavity. The effect of cylinder rotation on the isotherms is shown in Fig. 11. It was found that the thickness of the thermal boundary layer decreases with the increase in the rotational speed of the cylinder and thus improves the heat transfer process.

Also, when we take another value for Reynolds (*Re* = 100) Figs. 12 and 13, noticed how the heat transfer process is affected by an increase in rotational speed, as we notice an improvement in the heat transfer process with an increase in speed of cylinder.

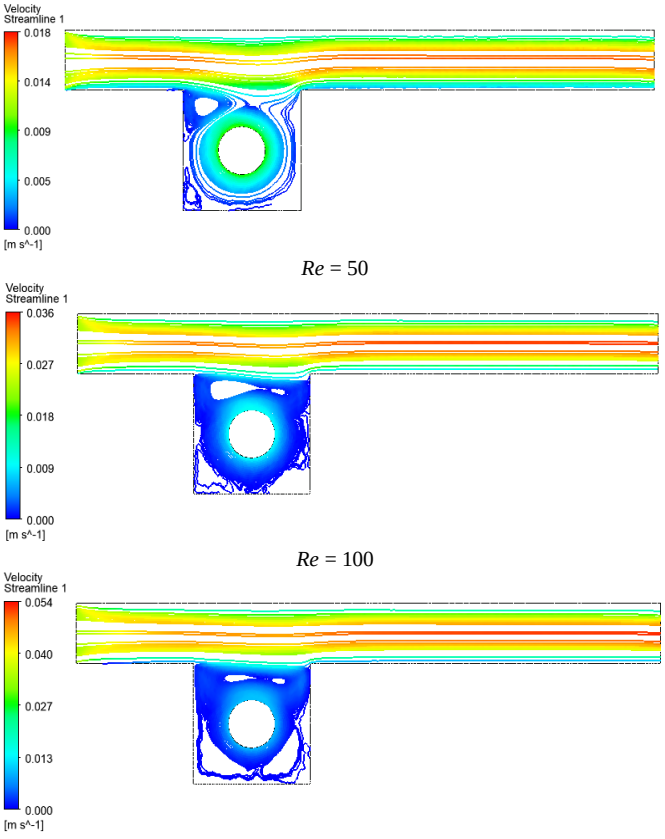

Fig. 6 Streamlines contours at *Ri* = 0.1, ω = 0.5 rad/sec.

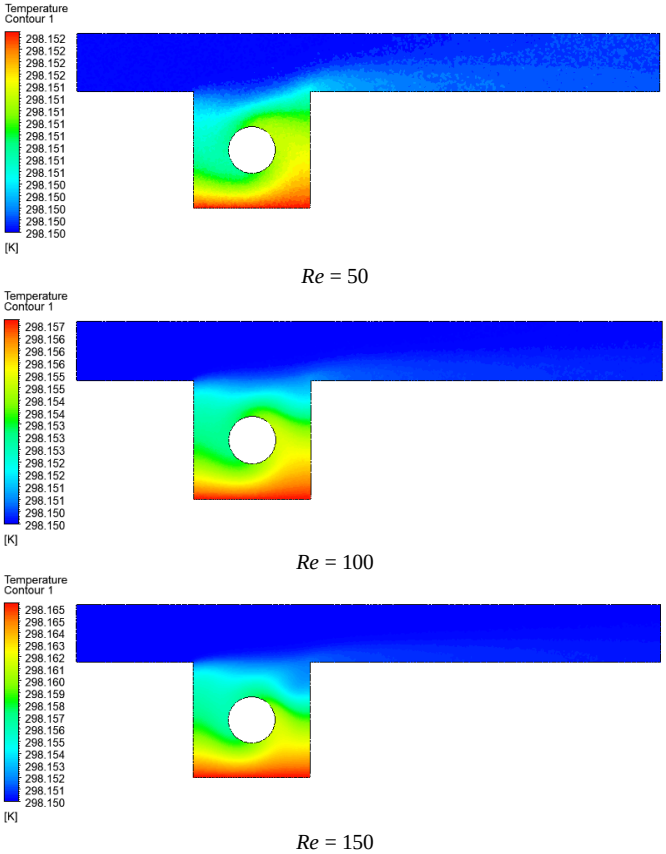

Fig. 7 Isothermal contours at *Ri* = 0.1, ω = 0.5 rad/sec.

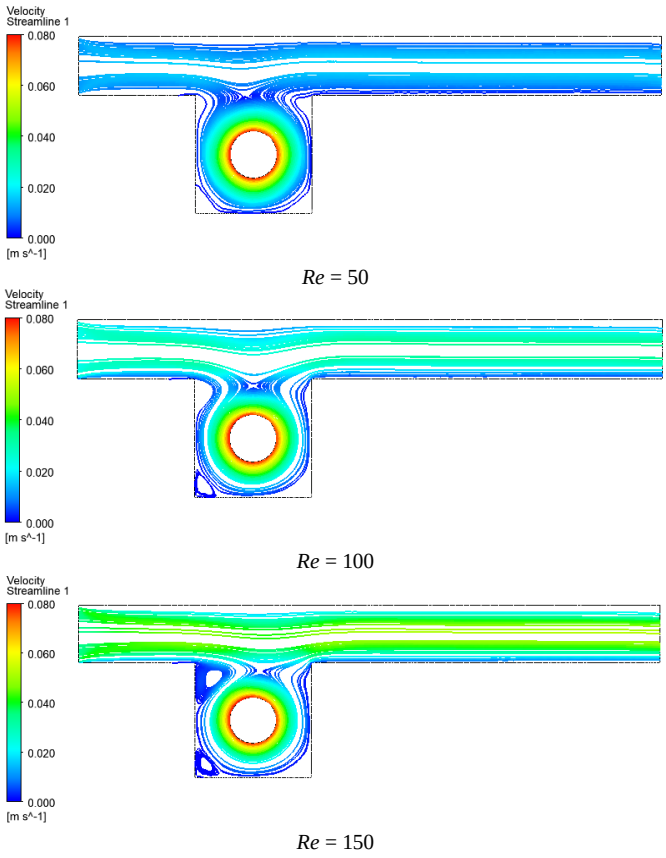

Fig. 8 Streamlines contours at Ri = 0.1, ω = 4 rad/sec.

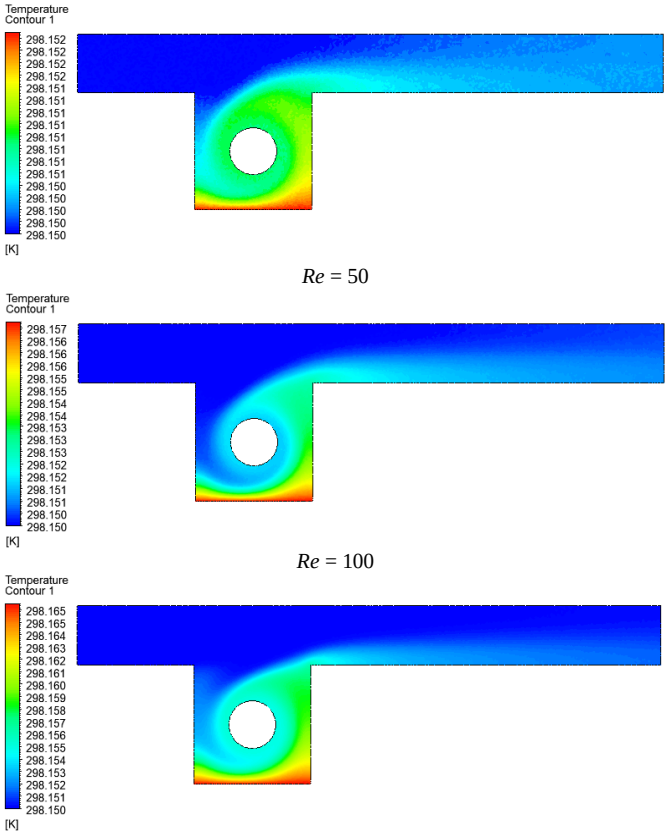

Fig. 9 Isothermal contours at Ri = 0.1, ω = 4 rad/sec.

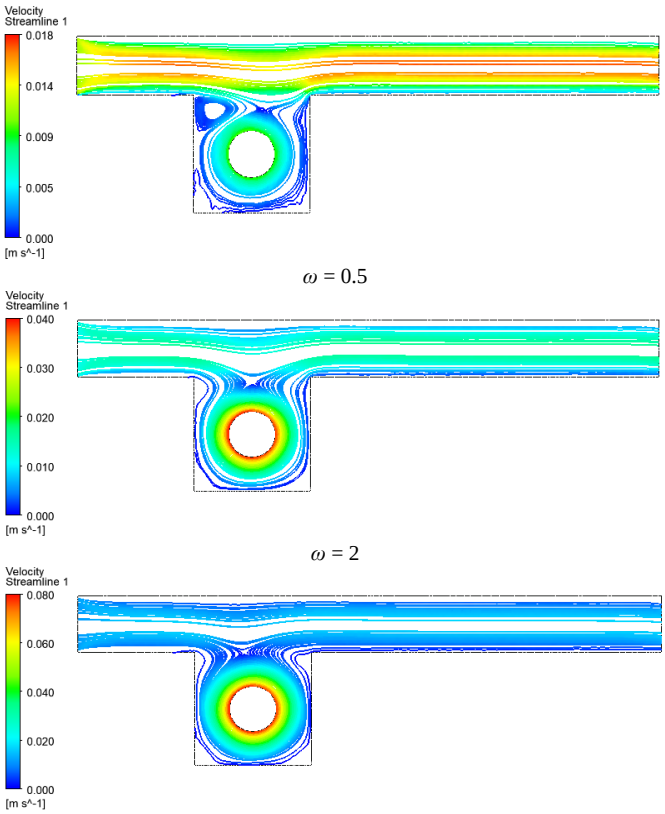

Fig. 10 Streamlines contour at Ri = 1, Re = 50.

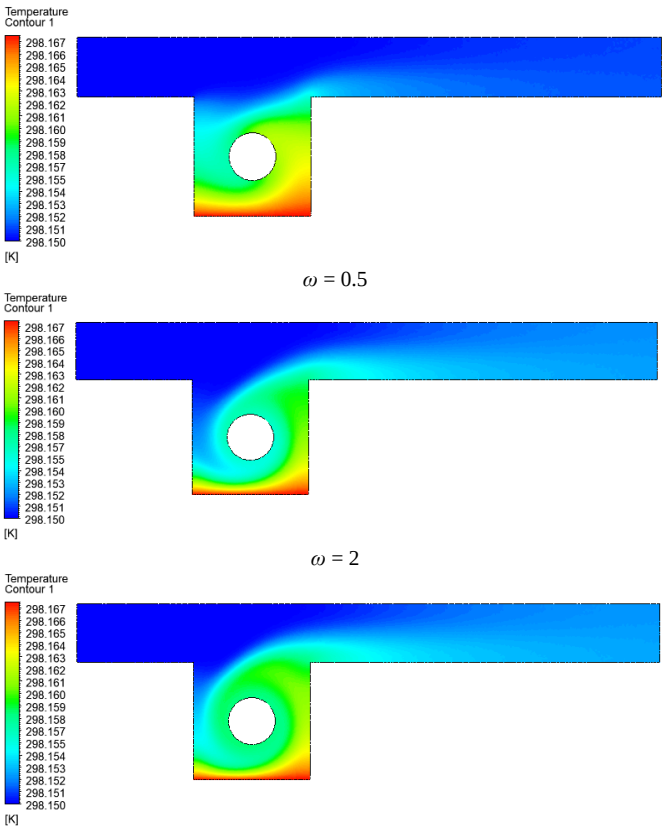

Fig. 11 Isothermal contours at Ri = 1, Re = 50.

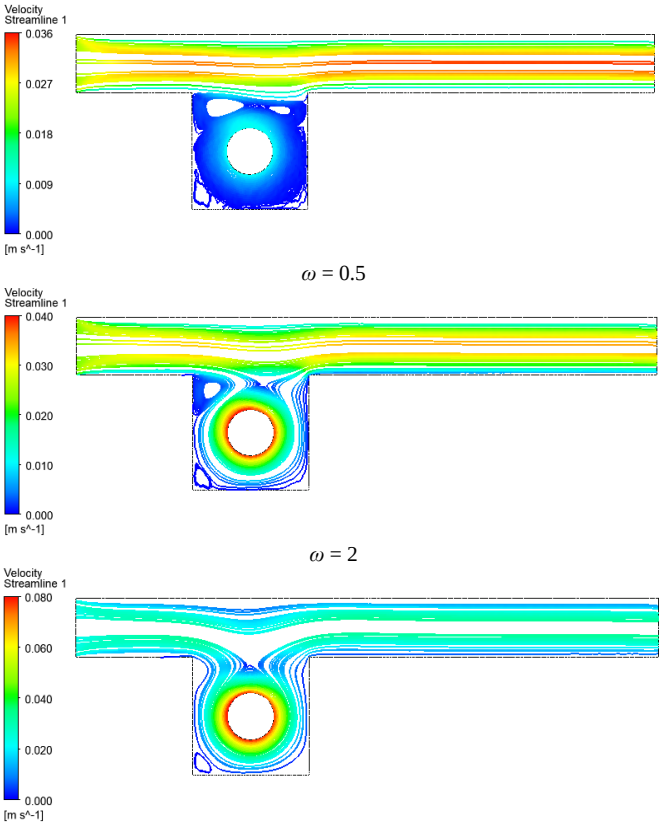

Fig. 12 Streamlines contour at *Re* = 100, *Ri* = 1.

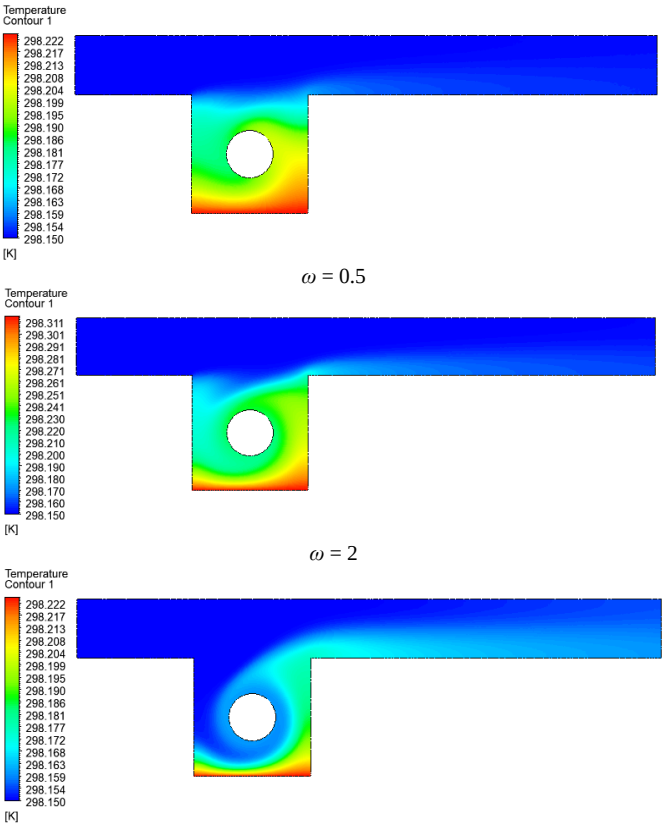

Fig. 13 Isothermal contours at *Re* = 100, *Ri* = 1.

4.2. Nusselt Number

Figures 14, 15 and 16 shows the variation of Nusselt number along the heated surface at different Richardson numbers, Reynolds numbers and angular velocities, respectively.

Based on the diagrams of the Fig. 14, we notice that with the increase in Richardson's values, the Nusselt values increase. As a result of increasing the effectiveness of free convection by increasing Richardson's number, and thus the heat transfer process improves for each of the two rotational speeds ω = 0.5, 4 rad/sec, However the Nusselt number at higher values when ω = 4 rad/sec.

Fig. 15, when ω = 0.5 rad/sec, the Nusselt values are good at low Reynolds numbers *Re* = 50 and decrease with increase Reynolds Re = 100, 150, but when increase in the rotational speed of the cylinder ω = 4 rad/sec, for Reynolds values of 50 and 100 results in an increase in the Nusselt values, and decreases when Reynolds is increased to 150.

Through Fig. 16, how the heat transfer process is affected by an increase in rotational speed? as we notice an improvement in the heat transfer process with an increase in speed, and noticed that the Nusselt values increase with the increase in the rotational speed of the cylinder. This is due to the increase in the effect of forced convection inside the cavity by increasing the speed of the cylinder.

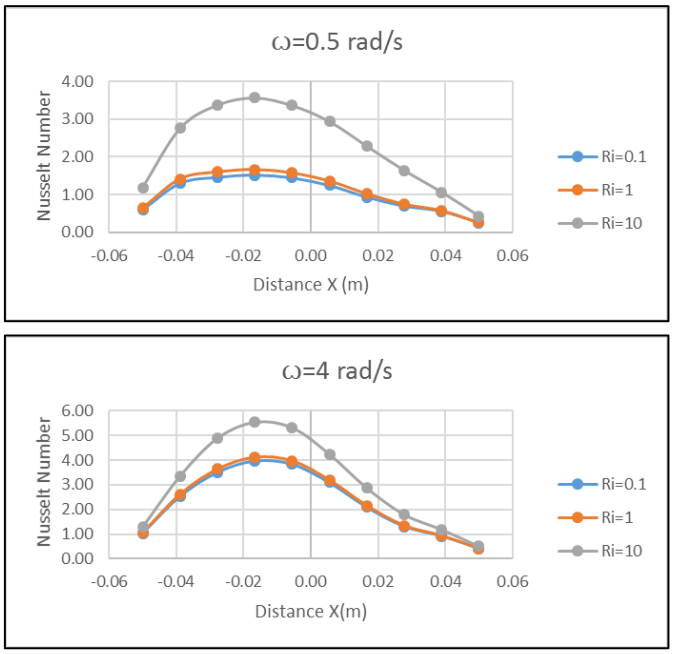

Fig. 14 Variation of Nusselt number along the heated surface at *Re* = 50.

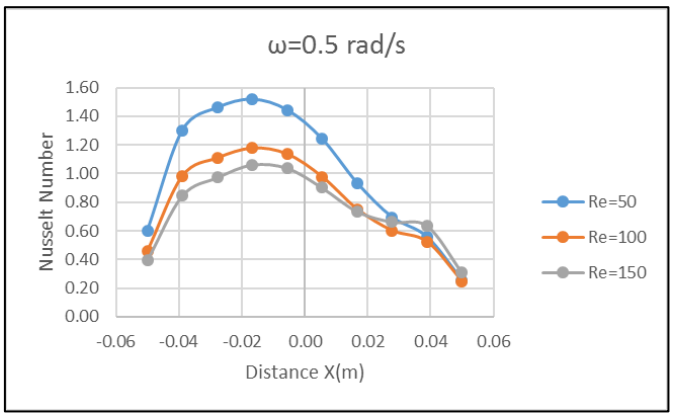

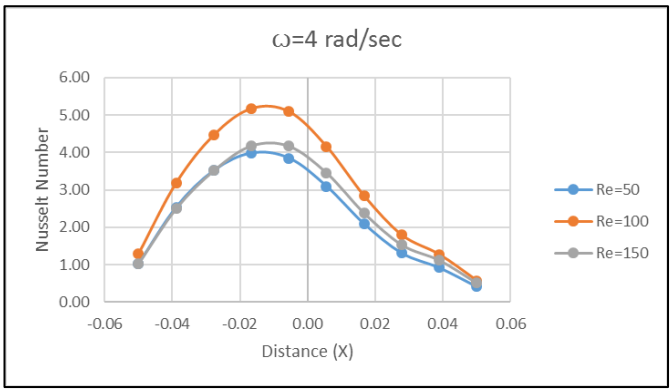

Fig. 15 Variation of Nusselt number along the heated surface at *Ri* = 0.1.

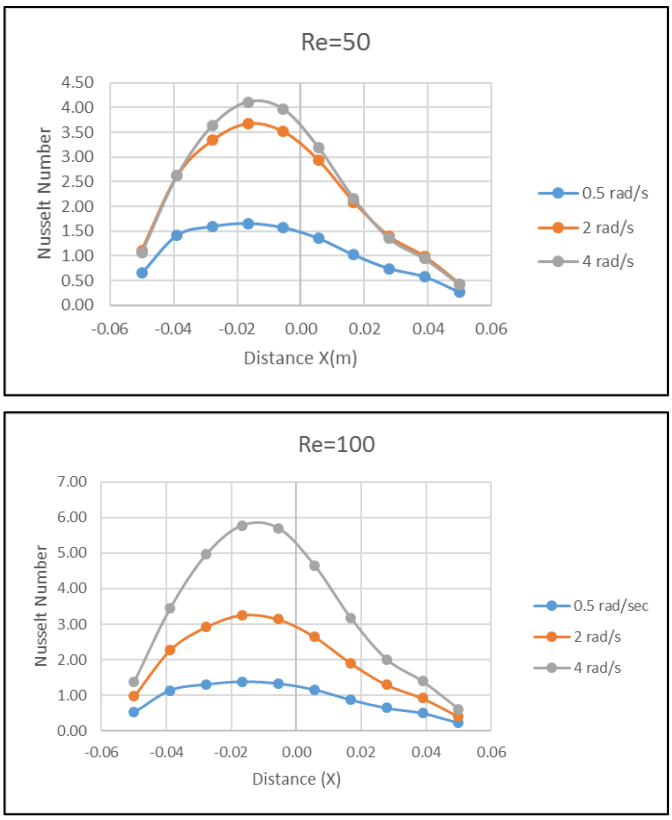

Fig. 16 Variation of Nusselt number along the heated surface at *Ri* = 1.

5. Conclusions

Numerical simulation has been carried out for the mixed convective flow over 2D square open cavity heated from below containing rotating cylinder. The effects of Reynolds number ($50 \leq Re \leq 150$), Richardson number ($0.1 \leq Ri \leq 10$), and cylinder rotation ($0.5 \leq \omega \leq 4$) rad/s.

1. The effect of the buoyancy becomes fixed for small *Ri* in the range $Ri < 1$ for all $Re \leq 150$.
2. Nusselt number increase with *Ri* for each value of *Re* and angular speed, when *Ri* is low the buoyancy is weak, force convective is dominate. At high *Ri* the Nu become high as the buoyancy force becomes stronger and mixed convection dominates.
3. As the angular speed increase, local Nusselt number increases for each value of Reynolds number.
4. It was found that the thickness of the thermal boundary layer decreases with the increase in the rotational speed of the cylinder and thus improves the heat transfer process.
5. At ω = 0.5 rad/s, the average heat transfer decrease with increase Reynolds number but for higher angular speed ω = 4 rad/s, there is slightly change of a value of the Nusselt number and its location with cylinder rotation.

Nomenclature		
Symbol	**Description**	**Unit**
D	Dimensional cylinder length	m
D_h	Hydraulic diameter	m
Gr	Grashof number	-
g	Gravitational acceleration	m/s^2
L	Length of the enclosure	m
Nu	Nusselt number	-
Pr	Prandtl number	-
Re	Reynolds number	-
Ri	Richardson number	-
T	Temperature	K
Th	Hot temperature	K
Ti	Inlet temperature	K
u, v	Cartesian velocity components	m/s
X, Y	Cartesian coordinates	-
k	Thermal conductivity of fluid	W/m. K
P	Pressure	N/m^2
Cp	Specific heat of air at constant pressure	J/kg. K
T_∞	Temperature of free stream	K
Greek Symbols		
Symbol	**Description**	**Unit**
α	Thermal diffusivity	m^2/s
β	Thermal expansion coefficient	1/K
υ	Kinematic viscosity	m^2/s
ρ	Density of the fluid	kg/m^3
ω	Angular velocity	rad/sec
μ	Dynamic viscosity	kg/m. s

References

[1] R. P. Garcia, S. R. Oliveira, and V. L. Scalon, "Thermal efficiency experimental evaluation of solar flat plate collectors when introducing convective barriers", Solar Energy, Vol. 182, pp. 278-285, 2019. https://doi.org/10.1016/j.solener.2019.02.048

[2] Y. Jiang, A. Poozesh, S. M. Marashi, R. Moradi, M. B. Gerdroodbary, A. Shafee, Z. Li and H. Babazadeh, "Effect of cavity back height on mixing efficiency of hydrogen multi-jets at supersonic combustion chamber", International Journal of Hydrogen Energy, Vol. 45, Issue 51, pp. 27828-27836, 2020. https://doi.org/10.1016/j.ijhydene.2020.07.001

[3] O. Manca, S. Nardini, K. Khanafer, and K. Vafai, "Effect of heated wall position on mixed convection in a channel with an open cavity", Numerical Heat Transfer, Part A: Applications, Vol. 43, Issue 3, pp. 259-282, 2003. https://doi.org/10.1080/10407780307310

[4] Y. Stiriba, F. X. Grau, J. A. Ferré, and A. Vernet, "A numerical study of three-dimensional laminar mixed convection past an open cavity", International Journal of Heat and Mass Transfer, Vol. 53, Issue 21-22, pp. 4997-4808, 2010. https://doi.org/10.1016/j.ijheatmasstransfer.2010.06.012

[5] G. Abdelmassih, A. Vernet, and J. Pallarés, "Numerical simulation of incompressible laminar flow in a three-dimensional channel with a cubical open cavity with a bottom wall heated", Journal of Physics Conference Series, Vol. 395, No. 012099, 2012. https://doi.org/10.1088/1742-6596/395/1/012099

[6] G. Abdelmassih, S. Varela, A. Vernet, and J. Pallarés, "DPIV experimental study of mixed convection in an open cavity", 10th International Symposium on Particle Image Velocimetry – PIV13, Delft, the Netherlands, July 1-3, 2013.

[7] M. M. Rahman, M. A. Alim, and M. A. H. Mamun, "Finite element analysis of mixed convection in a rectangular cavity with a heat-conducting horizontal circular cylinder", Nonlinear Analysis: Modelling and Control, Vol. 14, No. 2, pp. 217-247, 2009. https://doi.org/10.15388/NA.2009.14.2.14522

[8] K. Khanafer, and S. M. Aithal, "Laminar mixed convection flow and heat transfer characteristics in a lid driven cavity with a circular cylinder", International Journal of Heat and Mass Transfer, Vol. 66, pp. 200-209, 2013. https://doi.org/10.1016/j.ijheatmasstransfer.2013.07.023

[9] V. A. F. Costa, and A. M. Raimundo, "Steady mixed convection in a differentially heated square enclosure with an active rotating circular cylinder", International Journal of Heat and Mass Transfer, Vol. 53, Issue 5-6, pp. 1208-1219, 2010. https://doi.org/10.1016/j.ijheatmasstransfer.2009.10.007

[10] S. B. Paramane, and A. Sharma, "Numerical investigation of heat and fluid flow across a rotating circular cylinder maintained at constant temperature in 2-D laminar flow regime", International Journal of Heat and Mass Transfer, Vol. 52, Issue 13-14, pp. 3205-3216, 2009. https://doi.org/10.1016/j.ijheatmasstransfer.2008.12.031

[11] S. H. Hussain, and A. K. Hussein, "Numerical investigation of natural convection phenomena in a uniformly heated circular cylinder immersed in square enclosure filled with air at different vertical locations", International Communications in Heat and Mass Transfer, Vol. 37, Issue 8, pp. 1115-1126, 2010. https://doi.org/10.1016/j.icheatmasstransfer.2010.05.016

[12] F. Selimefendigil, and H. F. Öztop, "Effect of a rotating cylinder in forced convection of ferrofluid over a backward facing step", International Journal of Heat and Mass Transfer, Vol. 71, pp. 142-148, 2014. https://doi.org/10.1016/j.ijheatmasstransfer.2013.12.042

[13] D. Chatterjee, B. Mondal, and P. Halder, "Hydromagnetic mixed convective transport in a vertical lid-driven cavity including a heat conducting rotating circular cylinder", Numerical Heat Transfer, Part A: Applications, Vol. 65, Issue 1, pp. 48-65, 2014. https://doi.org/10.1080/10407782.2013.812399

[14] J. Burgos, I. Cuesta, and C. Salueña, "Numerical study of laminar mixed convection in a square open cavity", International Journal of Heat and Mass Transfer, Vol. 99, pp. 599-612, 2016. https://doi.org/10.1016/j.ijheatmasstransfer.2016.04.010